Study of a Bounded Jet Flow Considering the Initial Turbulence

(A Method of Approximate Calculations for the Mean Velocity Field)

Tsutomu NOZAKI and Masahiro NAKASHIMA*

(Received May 31, 1988)

ABSTRACT

Approximate calculations of the bounded jet have been carried out by adding an assumption which was already proposed by the authors for the diffusion width of the bounded jet to the velocity disribution on the center-plane of the bounded jet. In order to determine the parameter contained in the assumed velocity distribution function and to compare the results of our calculations with those of previous experiments, the experiments have been done, as an example, using a nozzle having an aspect ratio of 1. As a result, the isotach patterns of the bounded jet agree well with the experimental results regardless of the initial turbulence intensity and the downstream location.

1. Introduction

It has been found from the investigations by Foss and Jones[1], McCabe[2], Holdeman and Foss[3] and authors[4],[5], that a bounded jet flow is three-dimensional on account of the interaction between the boundary layer developing on the bounding plates and the free jet. It has been also clarified by the authors' experiments[4] for the nozzle aspect ratio of 3 that the bounded jet depends on not only the nozzle aspect ratio but also the nozzle shape and the initial turbulence intensity, and that the velocity in the free diffusion direction is well expressed by using the velocity distribution function[6] of the two-dimensional jet flow.

The authors have proposed an approximate calculation[5] for the velocity distribution on the jet center-plane from a point of view that the bounded jet comes from the interaction between the wall turbulence as the boundary layer developing on the bounding plates and the free turbulence as a jet.

The approximate calculations for the bounded jet flow considering the initial turbulence intensity, especially over the whole flow field of that flow, have not been carried out yet, so far as the authors are aware.

In this paper, the approximate calculations by the momentum integral equation are done over the whole flow field, by using the velocity distribution functions in the diffusion direction and on the center-plane. Furthermore, in order to compare the calculated results with the experimental ones, as an example, the experiments for the flow having the nozzle aspect ratio of 1 have been done, prescribing the nozzle shape and the initial turbulence intensity.

2. Approximate calculations

2. 1 Momentum integral equations

Schematic models of the velocity distribution of the bounded jet are shown in Fig.1. The origin O is taken at the center of the nozzle exit, the axis of x in the streamwise direction at the origin O and the axes

* Kagoshima National College of Technology, Hayato-chou, Aira-gun, Kagoshima 899-51.

of y and z perpendicular to the axis of x. Let z^* be the distance from the bounding plate. The xOy plane is defined as the mid-plane of the bounded jet, and the xOz plane is the center-plane. Therefore, the flow field from the bounding plate to the mid-plane is shown in Fig.1. Let U_3 be the velocity on jet center axis, U_3 the velocity on the mid-plane and U_z the velocity on the center-plane. Denoting by u, v and w the axial velocity components, the equations of motion and continuity are given by

$$u\frac{\partial u}{\partial x}+v\frac{\partial u}{\partial y}+w\frac{\partial u}{\partial z^*}=\frac{1}{\rho}\frac{\partial \tau_{xy}}{\partial y}+\frac{1}{\rho}\frac{\partial \tau_{xz}}{\partial z^*} \quad \cdots\cdots (1)$$

and

$$\frac{\partial u}{\partial x}+\frac{\partial v}{\partial y}+\frac{\partial w}{\partial z^*}=0, \quad \cdots\cdots (2)$$

respectively, using the conventional symbols and applying the boundary layer approximation. Let δ_2 be the boundary layer thickness[5] due to the interaction between the free turbulence and the wall turbulence, and H the distance from the bounding plate to the mid-plane. After integrating Eq. (1) from O to b with respect to y and from O to H with respect to z^*, the following momentum integral equation is obtained:

$$\int_0^{\delta_2}\int_0^b u\frac{\partial u}{\partial x}dydz^*+\int_0^{\delta_2}\int_0^b v\frac{\partial u}{\partial y}dydz^*+\int_0^{\delta_2}\int_0^b w\frac{\partial u}{\partial z^*}dydz^*+\int_{\delta_2}^H\int_0^{b_3} u_3\frac{\partial u_3}{\partial x}dydz^*$$
$$+\int_{\delta_2}^H\int_0^{b_3} v_3\frac{\partial u_3}{\partial y}dydz^*+\int_{\delta_2}^H\int_0^{b_3} w_3\frac{\partial u_3}{\partial z^*}dydz^*=\frac{1}{\rho}\int_0^{\delta_2}\int_0^b\frac{\partial \tau_{xy}}{\partial y}dydz^*+\frac{1}{\rho}\int_0^{\delta_2}\int_0^b\frac{\partial \tau_{xz}}{\partial z^*}dydz^*$$
$$+\frac{1}{\rho}\int_{\delta_2}^H\int_0^{b_3}\frac{\partial \tau_{xy3}}{\partial y}dydz^*+\frac{1}{\rho}\int_{\delta_2}^H\int_0^{b_3}\frac{\partial \tau_{xz3}}{\partial y^*}dydz^*, \quad \cdots\cdots (3)$$

considering that the jet width $2b$ is the function of x and z^*. In this equation, the variables having the subscript 3 are the values in the region of $\delta_2 \leqq z^* \leqq H$ and they are independent of z^*. Substituting Eq. (2) into Eq. (3), the following equation is obtained:

$$\frac{d}{dx}\int_0^{\delta_2}\int_0^b u^2dydz^*+\frac{d}{dx}\int_{\delta_2}^H\int_0^{b_3} u_3^2dydz^*=-\frac{1}{\rho}\int_0^{(b)_{z^*=0}}\tau_w dy, \quad \cdots\cdots (4)$$

where τ_w is the wall shear stress.

The velocities u_3 and u are assumed as

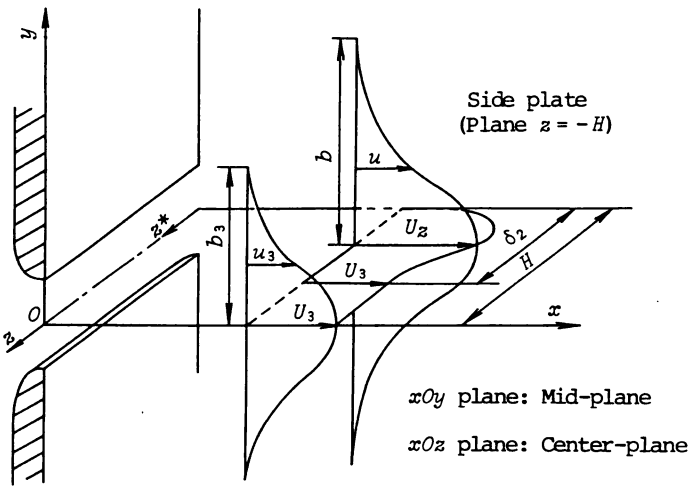

Fig.1 Schematic model of the flow

$$u_3 = U_3 f(\eta) \quad \cdots\cdots (5)$$

and

$$u = U_3 g(\zeta) f(\eta), \quad \cdots\cdots (6)$$

where $f(\eta)$ is the velocity distribution function[6] of the two-dimensional jet and is given as follows:

$$f(\eta) = 1 - 6\eta^2 + 8\eta^3 - 3\eta^4. \quad \cdots\cdots (7)$$

In this equation $\eta = (y - b_c)/(b - b_c)$ is given in the zone of flow establishment, denoting $2b_c$ the width of the inviscid core and $\eta = y/b$ in the zone of established flow. Furthermore, $g(\zeta)$ contained in Eq. (6) is the function[5] of velocity distribution on the jet center-plane and is given as follows, putting $\zeta_1 = z^*/\delta_1$ and $\zeta_2 = z^*/\delta_2$:

$$g(\zeta) = \zeta_1^{1/7}\left(\frac{8}{7} - \frac{\zeta_1}{7}\right) + k\zeta_2(1-\zeta_2)^3 \quad \cdots\cdots (8)$$

in the zone of $0 \leqq z^* < \delta_1$,

$$g(\zeta) = 1 + k\zeta_2(1-\zeta_2)^3 \quad \cdots\cdots (9)$$

in the zone of $\delta_1 \leqq z^* < \delta_2$, where δ_1 is the boundary layer thickness on the bounding plate. In Eqs. (8) and (9), k is the shape parameter of the velocity distribution expressing the extent of the interaction between the free turbulence and the wall turbulence and is determined only by the experiment.

Furthermore, τ_w in the right hand side of Eq. (4) is assumed as follows;

$$\tau_w = \tau_{w0} f^2(\eta), \quad \cdots\cdots (10)$$

using the wall shear stress on the jet center-plane τ_{wo} and the velocity distribution function in the diffusion direction $f(\eta)$. The stress τ_{wo} is given as;

$$\frac{\tau_{w0}}{\rho} = \alpha U_3^2 \left(\frac{U_3\delta_1}{\nu}\right)^{-1/4} \quad \cdots\cdots (11)$$

in the same way as the previous report[5] and α is given by 0.0225.

Consequently, Eq. (4) becomes

$$\frac{d}{dx}\left\{U_3^2 \int_0^{\sigma_2}\int_0^{b} f^2(\eta) g^2(\zeta) dy dz^*\right\} + \frac{d}{dx}\left\{U_3^2 \int_{\sigma_2}^{H}\int_0^{b_3} f^2(\eta) dy dz^*\right\}$$
$$= -\frac{\tau_{w0}}{\rho}\int_0^{(b_2)_{z^*=0}} f^2(\eta) dy. \quad \cdots\cdots (12)$$

On the basis of the structure of the jet flow, the approximate calculations are done both in the zone of flow establishment and in the zone of established flow.

2. 2 The zone of flow establishment

In this region it is assumed that the width of the inviscid core $2b_c$ and the width of the jet $2b$ at the outer edge of the boundary layer are the same as those in the two-dimensional jet respectively and that δ_1 is equal to δ_2. Furthermore, as U_3 in Eqs. (5) and (6) are equal to the velocity at the nozzle exit U_0, Eq. (12) becomes

$$\frac{d}{dx}\int_0^{\sigma_1} g^2(\zeta)\left(\frac{5}{7}b_c + \frac{2}{7}b\right) dz^* + \frac{d}{dx}\int_{\sigma_1}^{H}\left(\frac{5}{7}b_{c2} + \frac{2}{7}b_2\right) dz^*$$
$$= -\alpha\left(\frac{Re}{2}\right)^{-1/4}\left(\frac{\delta_1}{b_0}\right)^{-1/4}\left(\frac{5}{7}b_c + \frac{2}{7}b\right)_{z^*=0} \quad \cdots\cdots (13)$$

where $R_e = 2U_0 b_0/\nu$.

In the case of the two-dimensional jet, the following relation[6] has been obtained;

$$\frac{5}{7}b_{c2} + \frac{2}{7}b_2 = b_0 \quad \cdots\cdots (14)$$

from the conservation of momentum. Concerning the width of the inviscid core and the width of the jet in the boundary layer, they are assumed as follows;

$$b_c = b_{c2} h(\zeta_2) \quad \cdots\cdots (15)$$

and

$$b = b_2 h(\zeta_2), \quad \cdots\cdots (16)$$

using b_{c2}, b_2 and the function $h(\zeta_2)$. Finally, Eq. (13) reduces to

$$\frac{d}{dx}\int_0^{\sigma_1} h(\zeta_2) g^2(\zeta) dz^* - \frac{d\delta_1}{dx} = -\alpha \left(\frac{R_e}{2}\right)^{-1/4} \left(\frac{\delta_1}{b_0}\right)^{-1/4} h(0). \quad \cdots\cdots (17)$$

2. 3 The zone of established flow

In this region, the velocity on the jet center axis U_3 and the width of the jet at the outer edge of the boundary layer b_3 are different from those of the two-dimensional jet, respectively. Taking these facts into consideration, Eq. (12) becomes as follows;

$$\frac{d}{dx}\int_0^{\sigma_2} \frac{2}{7} U_3^2 b g^2(\zeta) dz^* + \frac{d}{dx}\int_{\sigma_2}^{H} \frac{2}{7} U_3^2 b_3 dz^* = -\frac{2}{7}\alpha U_3^2 \left(\frac{R_e}{2}\right)^{-1/4} \left(\frac{U_3}{U_0}\right)^{-1/4} \left(\frac{\delta_1}{b_0}\right)^{-1/4} (b)_{z^*=0}. \quad \cdots\cdots (18)$$

In this region, the jet width is assumed as

$$b = b_3 h(\zeta_2) \quad \cdots\cdots (19)$$

in the same way as the zone of flow establishment mentioned above. Therefore, Eq. (18) reduces to

$$\frac{d}{dx}\left\{\frac{2}{7} U_3^2 b_3 \int_0^{\sigma_2} h(\zeta_2) g^2(\zeta) dz^*\right\} + \frac{d}{dx}\left[\frac{2}{7} U_3^2 b_3 (H - \delta_2)\right]$$
$$= -\frac{2}{7}\alpha U_3^2 b_3 \left(\frac{R_e}{2}\right)^{-1/4} \left(\frac{U_3}{U_0}\right)^{-1/4} \left(\frac{\delta_1}{b_0}\right)^{-1/4} h(0), \quad \cdots\cdots (20)$$

It is assumed that the momentum in the region of $\delta_2 \leqq z^* \leqq H$ is kept constant in the streamwise direction analogous to the two-dimensional jet. Furthermore, using the results[6] calculated from the momentum integral equation

$$\frac{2}{7} U_3^2 b_3 = U_0^2 b_0 \quad \cdots\cdots (21)$$

in the zone of established flow of the two-dimensional jet, Eq. (20) reduces to

$$\frac{d}{dx}\int_0^{\sigma_2} h(\zeta_2) g^2(\zeta) dz^* - \frac{d\delta_2}{dx} = -\alpha \left(\frac{R_e}{2}\right)^{-1/4} \left(\frac{U_3}{U_0}\right)^{-1/4} \left(\frac{\delta_1}{b_0}\right)^{-1/4} h(0). \quad \cdots\cdots (22)$$

2. 4 The width of the jet in the boundary layer

The function $h(\zeta_2)$ expressing the variation of the jet width in the z^* direction and contained in Eqs. (15), (16) and (19) is assumed as

$$h(\zeta_2) = a + b\zeta_2 + c\zeta_2^2,$$

considering the experimental results. The following boundary conditions are assumed for $h(\zeta_2)$:

$$\zeta_2 = 1 \ ; \ h(1) = 1, \ h'(1) = 0.$$

The polynomial of ζ_2 satisfying these boundary conditions is obtained as follows:

$$h(\zeta_2) = (a-1)(1-\zeta_2)^2 + 1, \quad \cdots\cdots (23)$$

leaving one unknown parameter a. The variable a contained in this function $h(\zeta_2)$ means the ratio of the jet width at the outer edge of the boundary layer b_3 to the apparent jet width at the bounding plate $(b)_{z^*=0}$.

After substituting Eq. (23) to Eq. (17) or Eq (22), the following ordinary differential equation with respect to the variable a is obtained :

$$f_1(x)\frac{da}{dx}+f_2(x)a+f_3(x)=0, \quad \cdots\cdots (24)$$

where $f_1(x)$, $f_2(x)$ and $f_3(x)$ are given by

$$f_1(x)=\frac{9604}{38295}\delta_1,$$

$$f_2(x)=\frac{9604}{38295}\frac{d\delta_1}{dx}+\alpha\left(\frac{R_e}{2}\right)^{-1/4}\left(\frac{\delta_1}{b_0}\right)^{-1/4}$$

and

$$f_3(x)=-\frac{1581}{4255}\frac{d\delta_1}{dx}$$

in the zone of the flow establishment and

$$f_1(x)=\delta_2\left[\left\{-\frac{104}{12765}\left(\frac{\delta_1}{\delta_2}\right)^3+\frac{16}{345}\left(\frac{\delta_1}{\delta_2}\right)^2-\frac{25}{207}\frac{\delta_1}{\delta_2}+\frac{1}{3}\right\}+k\left\{\frac{8}{9975}\left(\frac{\delta_1}{\delta_2}\right)^7-\frac{4}{645}\left(\frac{\delta_1}{\delta_2}\right)^6\right.$$
$$\left.+\frac{8}{387}\left(\frac{\delta_1}{\delta_2}\right)^5-\frac{10}{261}\left(\frac{\delta_1}{\delta_2}\right)^4+\frac{40}{957}\left(\frac{\delta_1}{\delta_2}\right)^3-\frac{4}{165}\left(\frac{\delta_1}{\delta_2}\right)^2+\frac{1}{21}\right\}+\frac{1}{495}k^2\Big],$$

$$f_2(x)=\frac{d\delta_1}{dx}\left[\left\{-\frac{104}{4255}\left(\frac{\delta_1}{\delta_2}\right)^2+\frac{32}{345}\frac{\delta_1}{\delta_2}-\frac{25}{207}\right\}+k\left\{\frac{8}{1425}\left(\frac{\delta_1}{\delta_2}\right)^6-\frac{8}{215}\left(\frac{\delta_1}{\delta_2}\right)^5+\frac{40}{387}\left(\frac{\delta_1}{\delta_2}\right)^4\right.\right.$$
$$\left.\left.-\frac{40}{261}\left(\frac{\delta_1}{\delta_2}\right)^3+\frac{40}{319}\left(\frac{\delta_1}{\delta_2}\right)^2-\frac{8}{165}\frac{\delta_1}{\delta_2}\right\}\right]+\frac{d\delta_2}{dx}\left[\left\{\frac{208}{12765}\left(\frac{\delta_1}{\delta_2}\right)^3-\frac{16}{345}\left(\frac{\delta_1}{\delta_2}\right)^2+\frac{1}{3}\right\}\right.$$
$$\left.+k\left\{-\frac{16}{3325}\left(\frac{\delta_1}{\delta_2}\right)^7+\frac{4}{129}\left(\frac{\delta_1}{\delta_2}\right)^6-\frac{32}{387}\left(\frac{\delta_1}{\delta_2}\right)^5+\frac{10}{87}\left(\frac{\delta_1}{\delta_2}\right)^4-\frac{80}{957}\left(\frac{\delta_1}{\delta_2}\right)^3+\frac{4}{165}\left(\frac{\delta_1}{\delta_2}\right)^2+\frac{1}{21}\right\}+\frac{1}{495}k^2\right]$$
$$+\frac{dk}{dx}\delta_2\left\{\frac{8}{9975}\left(\frac{\delta_1}{\delta_2}\right)^7-\frac{4}{645}\left(\frac{\delta_1}{\delta_2}\right)^6+\frac{8}{387}\left(\frac{\delta_1}{\delta_2}\right)^5-\frac{10}{261}\left(\frac{\delta_1}{\delta_2}\right)^4+\frac{40}{957}\left(\frac{\delta_1}{\delta_2}\right)^3-\frac{4}{165}\left(\frac{\delta_1}{\delta_2}\right)^2+\frac{1}{21}+\frac{2}{495}k\right\}$$
$$+\alpha\left(\frac{R_e}{2}\right)^{-1/4}\left(\frac{U_3}{U_0}\right)^{-1/4}\left(\frac{\delta_1}{b_0}\right)^{-1/4}$$

and

$$f_3(x)=\frac{d\delta_1}{dx}\left[\left\{\frac{104}{4255}\left(\frac{\delta_1}{\delta_2}\right)^2-\frac{32}{345}\frac{\delta_1}{\delta_2}\right\}+k\left\{-\frac{8}{1425}\left(\frac{\delta_1}{\delta_2}\right)^6+\frac{8}{215}\left(\frac{\delta_1}{\delta_2}\right)^5-\frac{4}{43}\left(\frac{\delta_1}{\delta_2}\right)^4+\frac{28}{261}\left(\frac{\delta_1}{\delta_2}\right)^3-\frac{16}{319}\left(\frac{\delta_1}{\delta_2}\right)^2\right\}\right]$$
$$+\frac{d\delta_2}{dx}\left[\left\{-\frac{208}{12765}\left(\frac{\delta_1}{\delta_2}\right)^3+\frac{16}{345}\left(\frac{\delta_1}{\delta_2}\right)^2+\frac{2}{3}\right\}+k\left\{\frac{16}{3325}\left(\frac{\delta_1}{\delta_2}\right)^7-\frac{4}{129}\left(\frac{\delta_1}{\delta_2}\right)^6+\frac{16}{215}\left(\frac{\delta_1}{\delta_2}\right)^5-\frac{7}{87}\left(\frac{\delta_1}{\delta_2}\right)^4\right.\right.$$
$$\left.\left.+\frac{32}{957}\left(\frac{\delta_1}{\delta_2}\right)^3+\frac{11}{210}\right\}+\frac{3}{1540}k^2\right]+\frac{dk}{dx}\delta_2\left\{-\frac{8}{9975}\left(\frac{\delta_1}{\delta_2}\right)^7+\frac{4}{645}\left(\frac{\delta_1}{\delta_2}\right)^6-\frac{4}{215}\left(\frac{\delta_1}{\delta_2}\right)^5+\frac{7}{261}\left(\frac{\delta_1}{\delta_2}\right)^4\right.$$
$$\left.-\frac{16}{957}\left(\frac{\delta_1}{\delta_2}\right)^3+\frac{11}{210}+\frac{3}{770}k\right\}-\frac{d\delta_2}{dx}$$

in the zone of established flow, respectively.

3. Experimental results and discussion

As explained in the previous report[5], in order to carry out the approximate calculations mentioned above, it is necessary to determine previously the shape parameter k contained in the velocity distribution function on the jet center-plane in each case of the nozzle aspect ratio. Therefore, the following experiments were done for the flow having the nozzle aspect ratio of 3, as an example. The experiments were performed prescribing the nozzle shape and the initial turbulence intensity T_0 because the bounded jet depends strongly upon these factors, which has been found from the authors' experiments[4]. The EN-type nozzle where the bounding plates from both walls of the nozzle part was used. The initial turbulence

intensity 0.012 was also prescribed as an example of small initial turbulence intensity and $T_0=0.081$ for large one.

3. 1 The velocity distribution on the jet center-plane

The experimental results of the velocity distribution on the jet center-plane are shown in Fig.2. The velocity excess, which means that the velocity near the bounding plates becomes larger than that in the middle part of the flow, is hardly recognized regardless of T_0 and the downstream location x/b_0. Furthermore, in the case of small initial turbulence intensity the flow in the vicinity of the bounding plates is displaced fairly by the interaction between the free turbulence and the wall turbulence.

The decay of the velocity on the jet center axis in the streamwise direction is shown in Fig.3. The velocity decay[7] for the two-dimensional jet flow is also shown in the same figure for a comparison. In the case of small initial turbulence intensity, the velocity tends to decay in the same way as that in the two-dimensional jet flow, whereas for large initial turbulence intensity the tendency of the velocity decay are considerably different from that in the two-dimensional jet flow.

It can be seen from Figs.2 and 3 that in the case of small initial turbulence intensity the fluid displaced by the bounding plates is transferred considerably to the diffusion direction as well as to the z^*-direction. As a result, the decay of velocity on the jet center axis becomes similar to that of the two-dimensional jet flow. On the other hand, in the case of large intial turbulence intensity the fluid displaced by the bounding plates is moved mainly to z^*-direction and then accelerates the flow near the mid-plane. After all the velocity on the jet center axis decays more slowly than that of the two-dimensional jet flow.

3. 2 The boundary layer thickness and the shape parameter

In order to calculate the boundary layer thickness δ_1 by means of the same method as the previous report[5], in the downstream location far from the zone of flow establishment the decay of the velocity on the jet center axis is given by the following empirical equations :

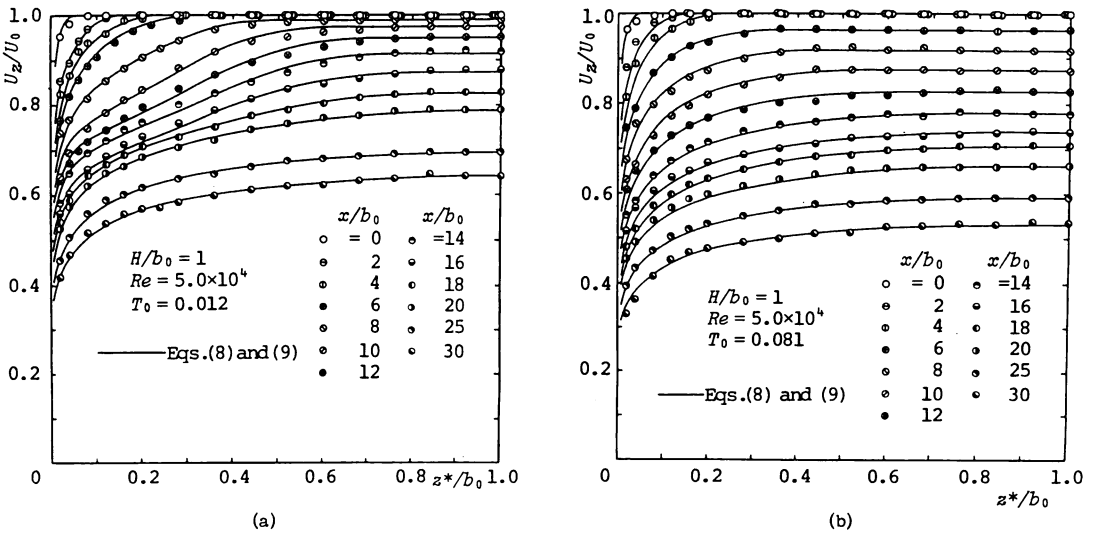

Fig.2 Velocity distribution on the jet center-plane

$$\frac{U_3}{U_0}=1.0+8.43\times10^{-4}\left(\frac{x}{b_0}-6.0\right)-1.80\times10^{-3}\left(\frac{x}{b_0}-6.0\right)^2+4.73\times10^{-5}\left(\frac{x}{b_0}-6.0\right)^3 \quad \cdots(25)$$

for $T_0=0.012$,

$$\frac{U_3}{U_0}=1.0-1.75\times10^{-2}\left(\frac{x}{b_0}-4.0\right)-5.49\times10^{-4}\left(\frac{x}{b_0}-4.0\right)^2+2.07\times10^{-5}\left(\frac{x}{b_0}-4.0\right)^3 \quad \cdots\cdots(26)$$

for $T_0=0.082$. In these equations the length of the zone of flow establishment is $x/b_0=6.0$ for $T_0=0.012$ and $x/b_0=4.0$ for $T_0=0.081$, respectively. The results of δ_1 calculated by using those equations are shown in Fig.4. The thickness δ_1 reaches the mid-plane in the region of $x/b_0>19.0$ for $T_0=0.012$ or $x/b_0>17.3$ for $T_0=0.081$ and then we put $\delta_1/b_0=1$.

The interaction thickness δ_2 on account of the interaction between the wall turbulence and the free turbulence is also shown in Fig.4. The definition of δ_2 is similar to that in the previous report[5]. For small initial turbulence intensity, δ_2 is expressed empirically by the following formula :

$$\frac{\delta_2}{b_0}=-7.99\times10^{-1}+2.85\times10^{-1}\left(\frac{x}{b_0}\right)-1.81\times10^{-2}\left(\frac{x}{b_0}\right)^2+4.23\times10^{-4}\left(\frac{x}{b_0}\right)^3 \quad \cdots\cdots(27)$$

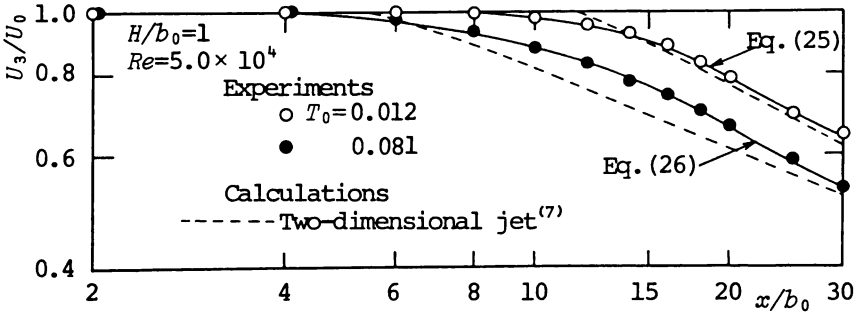

Fig.3 Decay of the jet center axis velocity

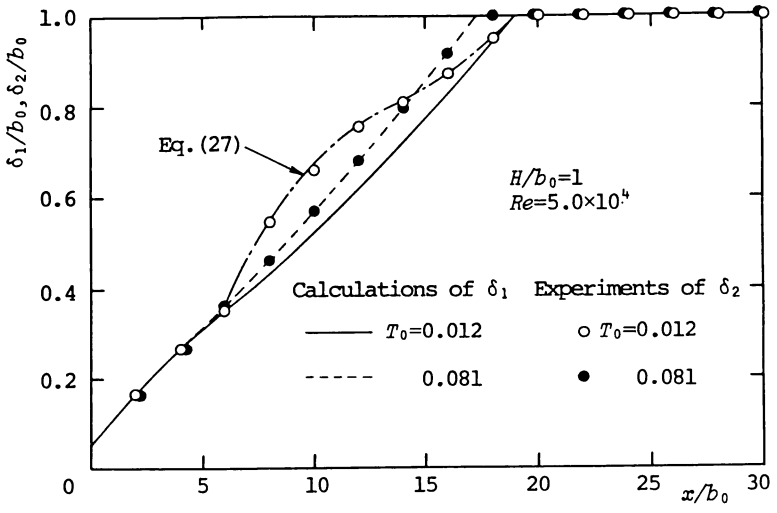

Fig.4 Variations of δ_1 and δ_2

in the region of $6.0<x/b_0<19.0$ and in the other region we put $\delta_2=\delta_1$. In the case of large initial turbulence intensity, $\delta_2=\delta_1$ is obtained everywhere because the effect of the bounding plates on the flow is greater than that of the diffusion.

The calculated results of the shape parameter k contained in the function $g(\zeta)$ are shown in Fig.5, by using the velocity distribution on the jet center-plane as shown in Fig.2 and the thicknesses δ_1 and δ_2 as shown in Fig.4. In the case of $T_0=0.012$, k is expressed as follows:

$$k=2.76-5.98\times10^{-1}\left(\frac{x}{b_0}\right)+2.28\times10^{-2}\left(\frac{x}{b_0}\right)^2+5.82\times10^{-5}\left(\frac{x}{b_0}\right)^3 \quad \cdots\cdots\cdots\cdots (28)$$

in the region of $6.0<x/b_0<19.0$ and $k=0$ is obtained for $19.0<x/b_0$. In the case of $T_0=0.081$, $k=0$ is obtained throughout the range of this experiment.

Considering together the results as shown in Figs.4 and 5, for small turbulence intensity the displacement effect from the bounding plates is more amplified than that of the ordinary boundary layer flow in the region of $6.0<x/b_0<19.0$ and then k has the negative value. Therefore, in this zone, the effect of the both bounding plates does not reach the jet mid-plane yet. However, in the downstream region far from this location δ_1 and δ_2 reach the mid-plane as shown in Fig.4 and $k=0$ is given. In the case of the large turbulence intensity, the effect of the both bounding plates appears at the upper downstream location. Therefore, $\delta_1=\delta_2$ and $k=0$ are obtained over the whole downstream location.

3. 3 The isotach pattern

The isotach patterns in each downstream location are shown in Figs.6 and 7. It can be seen from these figures that at $x/b_0=10$ the velocity in the vicinity of the plate is higher than that on the jet mid-plane regardless of T_0. At further downstream location the velocity in the vicinity of the plate decreases because the effect of the bounding plates appears gradually and then the velocity shows the maximum value on the mid-plane in $x/b_0=30$. These phenomena are recognized more clearly in the case of $T_0=0.081$.

The ordinary differential equation (24) for the variable a expressing the development of the jet width in the vicinity of the bounding plate is solved by the Runge-Kutta-Gill method, using the experimental results mentioned above. For the initial value of the variable a, $a=1$ is given considering the fact that the jet width $2b$ is equal to the nozzle width $2b_0$ at the nozzle exit. The variation of a in the streamwise

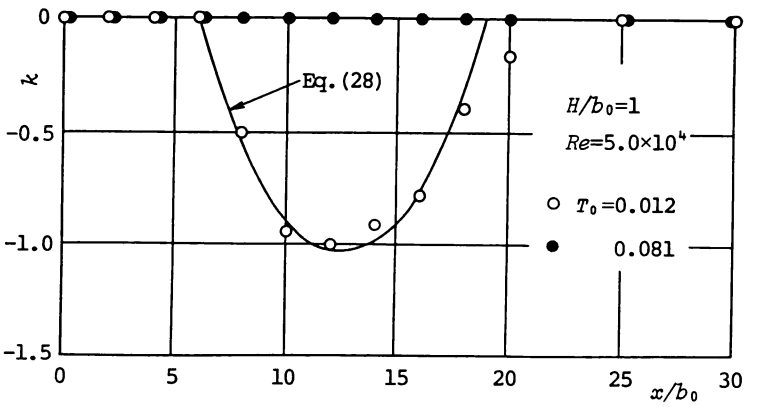

Fig.5 Shape parameter k

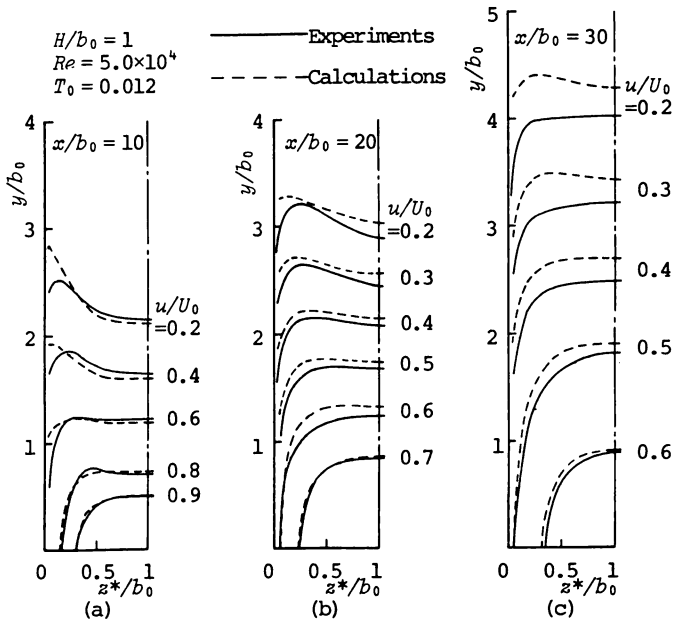

Fig.6 Isotach patterns (T_0=0.012)

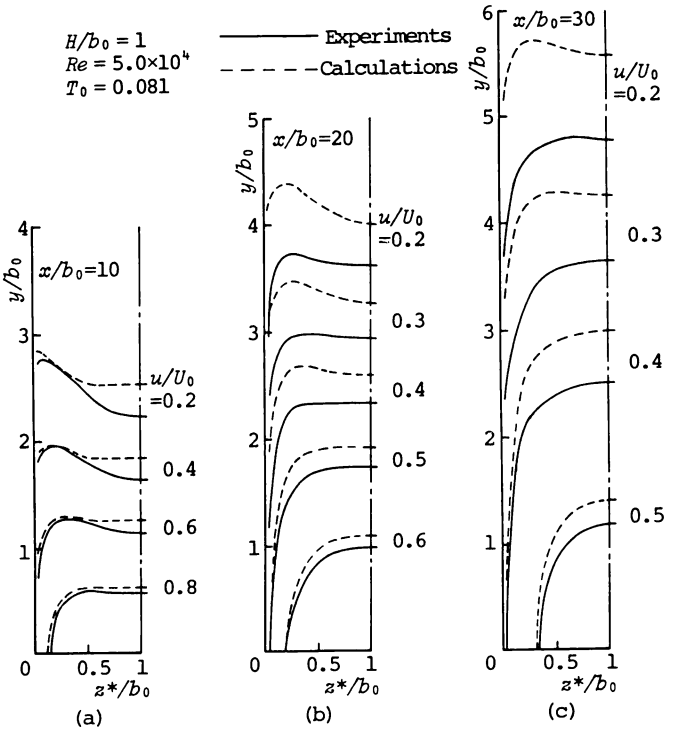

Fig.7 Isotach patterns (T_0=0.081)

direction is shown in Fig.8.

In the zone of flow establishment, the variable a has 1.2 approximately in spite of T_0. This fact means that in this region the jet width in the vicinity of the bounding plate is 1.2 times as large as that on the mid-plane. Furthermore, the fact that the variable a is almost constant in this region corresponds to that the velocity distribution in the boundary layer as shown in Fig.2 is similar each other.

The variable a increases gradually in the zone of established flow. The aspect of the variation of a is remarkable in the case of $T_0=0.012$, whereas a varries little for $T_0=0.081$. This corresponds to the following fact. In the case of the small initial turbulence intensity, the effect of the displacement in the center-plane becomes large and the displaced fluid is transferred to the diffusion direction. As a result, the jet tends to spread fairly in the vicinity of the bounding plates rather than in the mid-plane.

The variable a decreases in the downstream direction after having the maximum value. As mentioned in section 3.1, in this region the distance between the bounding plates contrary to the jet width becomes narrow. Therefore, the fluid displaced by the bounding plates reaches the mid-plane easily. As a result, the variable a decreases and the jet width in the vicinity of the bounding plates becomes to be almost equal to that on the jet mid-plane.

In the case of small initial turbulence intensity, the variation of a corresponds well to that of the secondary flow in the bounded jet reported by Holdeman-Foss[3], and this means the initiation, the development and the decay of the secondary flow. For large intial turbulence intensity, however, as mentioned above the flow field becomes narrow relatively so that the diffusion of the jet tends to be limited and the secondary flow begins to decay before it develops sufficiently.

The isotach patterns are obtained by using the variable a and the velocity distribution functions $g(\zeta)$ and $f(\eta)$. These calculations are shown by the broken line in Figs.6 and 7. The calculations agree well with the experimental results shown by the solid line regardless of the downstream location for $T_0=0.012$ and at $x/b_0=10$ for $T_0=0.082$. Therefore, if only the velocity distribution on the jet center-plane is measured, the whole flow field will be able to be expected by using the approximate calculation mentioned in this paper whenever the calculations for the bounded jet flow having the various aspect ratio are carried out.

The streamwise variations of the momentum obtained by the experimental and calculated results of the isotach patterns as shown in Figs.6 and 7 are shown in Fig.9. They agree well with each other for the small initial turbulence intensity. In the case of large intensity they do well with at $x/b_0=10$, whereas not well at other locations.

Discussing these facts together, for small initial turbulence intensity the decay of the velocity on the jet center axis and the development of the jet width agree well with those of the two-dimensional jet flow, respectively. Consequently, the momentum of the bounded jet agrees with that of the two-dimensional jet. In the case of large initial turbulence intensity, the momentum tends not to be kept constant in the downstream direction because the increase of the jet width matching to the decay of the velocity on the jet center axis is not sufficient.

4. Conclusions

As a part of the investigations for the bounded jet flow, the approximate calculations for the whole flow field of the bounded jet flow is carried out by the integral method using the velocity distribution functions, which have been reported already, in the diffusion direction of the two-dimensional jet and on the jet center-plane of the bounded jet and introducing newly the function expressing the variation of the jet width

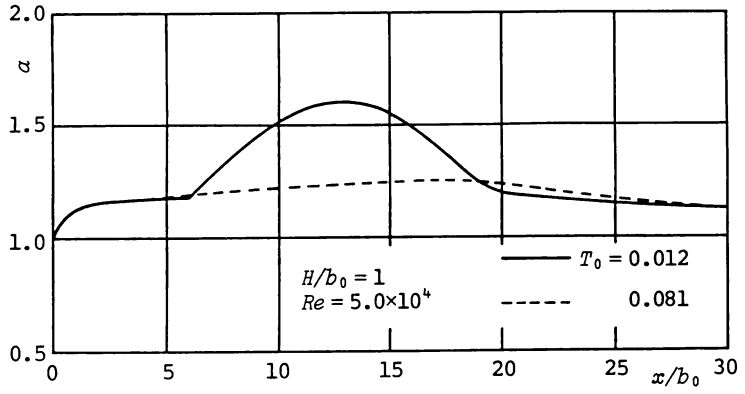

Fig.8 Variation of a

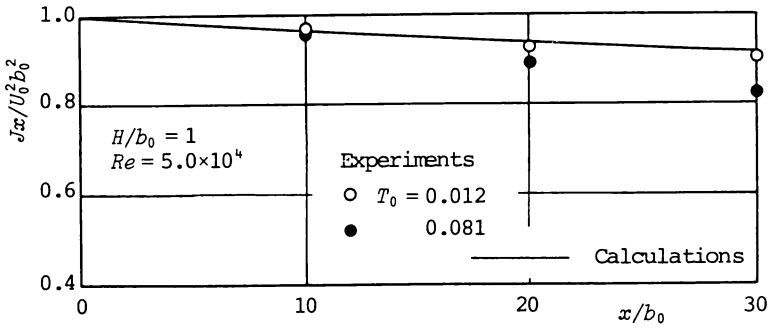

Fig.9 Variation of momentum

in the boundary layer. In order to compare with the calculated results, the experiments are done by using the nozzle having an aspect ratio of 1, as an example. As a result, in the case of the large initial turbulence intensity the calculated results agree with the experimental ones a little because the effect of the both bounding plates appears in addition to the interaction between the free turbulence and the wall turbulence and then the diffusion of the jet is also limited fairly. Generally speaking, however, the calculations obtained by the considerably simpler method agree well with the experimental results over the wide range of the flow. Therefore, it is possible to expect the mean velocity over the whole flow field by using this approximate calculations if only the velocity distribution on the jet center-plane is given.

References

(1) Foss, J.F. and Jones, J.B., Trans. ASME, Ser.D, 90-2(1968), 241.
(2) McCabe, A., Proc. Inst. Mech. Eng., 183-3H(1967-1968), 342.
(3) Holdeman, J.D. and Foss, J.F., Trans. ASME, Ser. I, 97-3(1975), 342.
(4) Nozaki, T., et. al., Bull. JSME, Vol.27, No.234(1984-12), 2730.
(5) Nakashima, M., et al., Bull. JSME, Vol.29, No.253(1986-7), 2042.
(6) Hatta, K. and Nozaki, T., Bull. JSME, Vol.18, No.118(1975-4), 349.
(7) Nozaki, T., et al., Bull. JSME, Vol.24, No.188(1981-2), 363.